The Diffusive Approximation for Eddy Fluxes in Baroclinically Unstable Jets

VALENTINA PAVAN*

Program in Atmospheric and Oceanic Sciences, Princeton University, Princeton, New Jersey

ISAAC M. HELD

Geophysical Fluid Dynamics Laboratory/NOAA, Princeton, New Jersey

(Manuscript received 23 January 1995, in final form 5 September 1995)

ABSTRACT

A series of statistically steady states for baroclinically unstable jets in a two-layer quasigeostrophic model is examined, in order to evaluate diffusive approximations to the eddy potential vorticity or heat fluxes. The flow is forced by thermal relaxation to an unstable "radiative equilibrium" temperature gradient. The statistically steady states are studied as a function of the width of the radiative equilibrium jet. A local diffusive "theory" for the eddy fluxes is obtained from integrations of a homogeneous, doubly periodic model with prescribed environmental potential vorticity gradients. The flux–gradient relationship generated by the homogeneous model predicts the magnitude and shape of the eddy fluxes in the unstable jet flows remarkably well, as long as the jet is not too narrow. These results confirm the relevance of diffusive closures for eddy potential vorticity and heat fluxes in such flows. For narrow jets that produce eddy fluxes with a half-width of one to two radii of deformation, this local theory underpredicts the fluxes.

1. Introduction

The development of a theory for the magnitude of the eddy fluxes and energy levels in the midlatitude troposphere remains a central problem in meteorology. In this paper, we approach this issue by studying the statistically steady states of a two-layer, quasigeostrophic model on a β plane. Since Phillips's (1956) pioneering work, it has been known that this model can reproduce some of the qualitative features of the midtropospheric flow. It is also well known that this model has serious deficiencies. Besides the constraint on vertical structure imposed by the two-layer assumption, the quasigeostrophic framework does not allow one to directly study the maintenance of the static stability of the troposphere. In spite of these limitations, we are confident that an understanding of this quasigeostrophic system is an important stepping stone to an understanding of more realistic models.

Two seemingly distinct pictures have often served as simple starting points for discussion of the eddy fluxes in idealized models of baroclinic instability and in the atmosphere: adjustment and diffusion. In an adjustment theory, the eddies are assumed to be constrained so as to generate a mean flow with certain properties. In its simplest form, as applied to the two-layer model, one assumes that the eddy fluxes remove the region of reversed potential vorticity (PV) gradient in the lower layer of the model (Stone 1978; Smagorinsky 1963). In the diffusive picture, the eddy PV flux is not only assumed to be directed down the mean PV gradient but also to have an amplitude that is determined by the local environment (Green 1970; Wiin-Nielsen and Sela 1971). These two pictures are not mutually exclusive. Both may be appropriate but in different parts of parameter space, or their ranges of validity may actually overlap. For example, a diffusive theory might predict a flux large enough, for any supercritical vertical shear, to overpower whatever restoring forces are present in the system and to reduce the shears to their critical values.

Authors who have addressed some of these issues include Harrison (1978), who examines the possibility of using a diffusive parameterization in the rather complex setting of a model of an ocean basin, and Vallis (1988), who discusses adjustment versus diffusive parameterizations in the context of a homogeneous quasigeostrophic model. Our work is most closely related to that of Panetta and Held (1988), who study the statistics of a baroclinically unstable flow as a function of the width of the unstable region.

A very useful technique for distinguishing between nonlocal adjustment and local diffusive theories is the

* Current affiliation: Reading University, Reading, England.

Corresponding author address: Dr. Isaac M. Held, GFDL, P.O. Box 308, Princeton, NJ 08542-0308.
E-mail: ih@gfdl.gov

© 1996 American Meteorological Society

Unauthenticated | Downloaded 07/26/21 04:37 AM UTC

study of baroclinically unstable jets as a function of the width of the jet. Specifically, suppose that one forces a two-layer model to develop baroclinic instability by relaxing the temperature (the interface height in the two-layer model) to

$$\theta(y) = \Delta\sigma \tanh\left(\frac{y}{\sigma}\right). \tag{1}$$

Here, σ is the width of the baroclinic jet in balance with this "radiative equilibrium" temperature field. We have chosen the temperature drop across the baroclinic zone proportional to σ so that the maximum strength of the radiative equilibrium jet is independent of σ. The relaxation timescale is fixed. As described more fully below, if the eddy fluxes are assumed to adjust the shear or temperature gradient to some critical value, then the flux must be proportional to σ^2. In contrast, a diffusive picture predicts that the flux will asymptote to a constant as $\sigma \to \infty$. Panetta and Held (1988) address this issue with a "wave-mean flow interaction" two-layer model, truncated so that only the zonal mean and a single zonal wavenumber are retained, and find that the diffusive prediction is correct. The rate at which the flow in their model can transport PV or heat does not grow without bound, even though the available potential energy in the radiative equilibrium state increases as σ^2. Our purpose in this paper is to reexamine this result with a more isotropically truncated two-layer model and to explore the implications for diffusive eddy flux closure schemes.

How does one compute or estimate the diffusivity to be used in a diffusive closure scheme? An important step is to isolate this problem in the setting of a horizontally homogeneous model with imposed environmental (time mean), horizontally uniform, PV gradients. The horizontal homogeneity is critical, since it prevents the eddies from modifying the environmental gradients, so that these gradients are external parameters; in principle, there is no convergence or divergence that can alter the time mean since the time-mean eddy fluxes are independent of horizontal position. If the flux is determined by the local environment in some way, rather than by more global constraints as in an adjustment theory, then the homogeneous model is the appropriate apparatus for "measuring" the diffusivity.

With radiative equilibrium temperatures given by (1), in the limit as $\sigma \to \infty$ the eddy statistics should approach those predicted by a homogeneous model in which the imposed mean temperature gradient is the radiative equilibrium gradient at the jet center. The results in Panetta and Held (1988) support this contention for the truncated model they consider. But if the fluxes or diffusivities obtained from the homogeneous model are only relevant in this limit, they will be of little meteorological (or oceanic) relevance. The hope is that the local relationship between the fluxes and the time-mean flow is qualitatively the same as that predicted by the homogeneous model, even for moderately narrow jets in which the mean flow is significantly modified by the eddies. We would like to understand the extent to which this is the case.

There are reasons to be pessimistic. The mean flow in the homogeneous model can have no horizontal shear, yet James and Gray (1986) have argued that the influence of barotropic shears on the statistics of baroclinic eddies is considerable. Also, in the homogeneous model the flow breaks down into multiple jets and storm tracks (Panetta 1993). This also occurs in inhomogeneous flows when the forcing is sufficiently slowly varying, but these structures complicate the comparison between the homogeneous and inhomogeneous flows.

After describing the models briefly in section 2, some statistically steady states of baroclinically unstable jets of various widths are described in section 3. These are compared to the predictions of the homogeneous model in section 4. Further discussion of eddy flux closures can then be found in the concluding section.

2. The models

The configuration and numerical scheme in our two-layer model is identical to that described by Lee and Held (1991). The model equations are

$$\partial_t q_i = -J(\psi_i, q_i) + S_i, \tag{2}$$

where

$$\begin{aligned} S_1 &= -H - \nu\nabla^4 q_1 \\ S_2 &= H + k_M\nabla^2\psi_2 - \nu\nabla^4 q_2 \\ H &= -k_T\left\{\frac{(\psi_1 - \psi_2)}{2} - \theta_{\text{eq}}(y)\right\}. \end{aligned} \tag{3}$$

The subscripts 1 and 2 refer to the upper and lower layers, respectively. The potential vorticities, streamfunctions, and velocities are linked by the following relations:

$$q_i = \beta y + \nabla^2\psi_i + (-1)^i\frac{\psi_1 - \psi_2}{2}, \tag{4}$$

$$(u_i, v_i) = (-\partial_y\psi_i, \partial_x\psi_i). \tag{5}$$

The flow is forced by the linear relaxation of the baroclinic streamfunction, $\theta = (\psi_1 - \psi_2)/2$, to its radiative equilibrium value θ_{eq}. Ekman damping of the vorticity is included in the lower layer, and biharmonic damping of the potential vorticity in both layers. The zonally averaged zonal flow is denoted by U. If there are no eddies, the flow will be zonal, U_2 will vanish, and

$$U_1 = U_{\text{eq}} = -2\frac{\partial\theta_{\text{eq}}}{\partial y} \equiv \operatorname{sech}^2\left(\frac{y}{\sigma}\right). \tag{6}$$

Unauthenticated | Downloaded 07/26/21 04:37 AM UTC

We have nondimensionalized by choosing the radius of deformation as the length scale and the maximum strength of the upper-level wind in radiative equilibrium, U_{eq}, as the velocity scale. In these units, a horizontally uniform vertical shear $U_1 - U_2 \equiv S$ is baroclinically unstable by Phillips's criterion, in the absence of damping, if $\beta - S/2 < 0$.

As a consequence of the simple linear form of the forcing in this model, the time-mean flow is a simple function of the eddy PV fluxes. In fact, if we average equation (2) in time, as well as in the zonal direction, and we neglect the contribution of the biharmonic diffusion term, we obtain that the lower-level zonal wind is proportional to the sum of the eddy potential vorticity fluxes in the two layers, while the deviation of the vertical shear of the zonal wind from its radiative value is proportional to the second derivative of the upper-layer flux:

$$U_2 = \frac{1}{k_M}(F_1 + F_2) \tag{7}$$

$$U_1 - U_2 = U_{eq} - \frac{2}{k_T}\frac{\partial^2 F_1}{\partial y^2} \tag{8}$$

where

$$F_i = \overline{v_i' q_i'} \,. \tag{9}$$

Here, an overbar refers to the zonal mean, while time means are understood in (7) and (8).

The domain is a reentrant channel with a length equal to 20π so that the smallest nonzero zonal wavenumber is 0.1. The width of the channel varies from experiment to experiment but is always large enough that there is essentially no eddy activity at the channel walls. The model is spectral in x and finite differenced in y. We retain 32 wavenumbers zonally and use five grid points per unit of length meridionally. While it would not be difficult to obtain some higher-resolution solutions, this modest resolution allows us to obtain numerous statistically steady states, including some in very wide channels. The nondimensional biharmonic diffusion coefficient is held at the value 10^{-3} throughout.

We also employ a doubly periodic model that is identical to that in Haidvogel and Held (1980). It is spectral in both dimensions and truncated at 64×64 waves so that there are 32 positive zonal wavenumbers, as in the channel model. The domain is a square of size 20π. In this homogeneous model, the domain-averaged winds and potential vorticity gradients in both layers are external parameters. The nondimensionalization is identical to that in the channel model. The mean upper-layer wind is set equal to S, and the lower-layer wind to zero. If $S = 1$, the vertical shear is equal to that in radiative equilibrium at the center of the jet in the channel model. The mean potential vorticity gradient is $\beta + S/2$ in the upper layer and $\beta - S/2$ in the lower layer. The biharmonic diffusivity has the same value as in the channel model. Both models are typically integrated for 1000–2000 time units, after discarding a spinup period, to obtain statistically steady states.

3. Channel model results

There are several parameters of interest in this model: β, which one can think of as a measure of the strength, or the supercriticality, of the jet; k_M, the strength of the Ekman damping; k_T, the strength of the thermal damping; and σ, the width of the radiative equilibrium jet. We have not been so ambitious as to attempt a full exploration of the parameter space. Instead, we focus on two particular choices for (β, k_M, k_T) and find solutions for a wide range of values of σ in these two cases. It is not clear how best to fit a two-layer model to the atmosphere; we have simply chosen two sets of parameters that represent moderately supercritical and strongly supercritical flows.

In case 1, we choose ($\beta = 0.25$, $k_M = 0.2$, $k_T = 1/30$). Figure 1a shows the resulting zonal-mean winds in the two layers, for the widths $\sigma = 5$ and 10. Two wider jets ($\sigma = 20$ and 40) are shown in Fig. 1b. Low-level westerlies are produced under the jet core, except in the widest case shown. For the wider jets, the storm track splits (Panetta 1993), and the eddy momentum fluxes directed into the different regions of enhanced eddy activity produce multiple regions of surface westerlies. Each region of surface westerlies is associated with a local maximum in vertical shear as well so that this structure is magnified in the upper-level winds. The strengths of the surface drag and radiative relaxation are such that the multiple jet structures are less well defined than in many of the cases described in Panetta (1993). The 1000-day averages are insufficient to obtain climatic statistics that are reasonably symmetric about the central axis, due to the slow timescales associated with these split jets.

Figure 2a shows the lower-layer potential vorticity gradient in these experiments. Two other cases, with even wider jets ($\sigma = 80$ and 160), have also been included. The value of this gradient in radiative equilibrium at the center of the jet is $\beta - 0.5 = -0.25$. In the narrowest cases only is there a substantial reduction in the strength of this gradient. The eddies clearly become less efficient at removing the negative gradient as the jet widens.

Figure 2b contains the eddy potential vorticity fluxes in the two layers for the six different jet widths. Notice that the width of the region of eddy activity as measured by these fluxes is somewhat narrower than the width of the jet. For $\sigma = 20$, the half-width of the flux is roughly 6. This flow is rather weakly unstable, in that the lower-layer potential vorticity gradient is negative near the center of the jet only. In fact, the regions of significant eddy PV fluxes correspond closely with the regions of negative PV gradient in Fig. 2a.

The second set of parameters that we study (case 2) is ($\beta = 0.10$, $k_M = 0.2$, $k_T = 0.01$). The smaller value

Unauthenticated | Downloaded 07/26/21 04:37 AM UTC

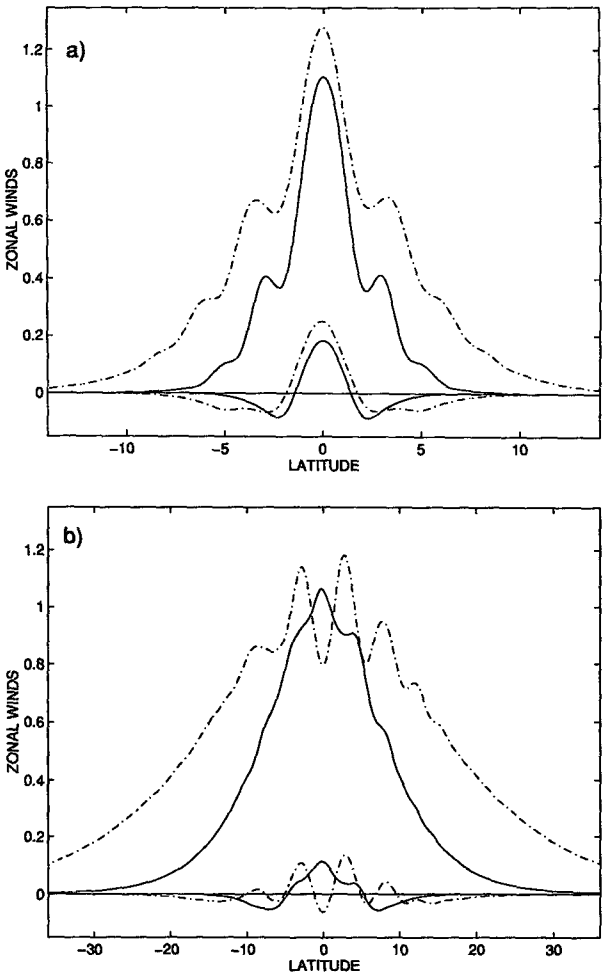

FIG. 1. Meridional profiles of the upper- and lower-layer time-mean zonal-mean wind for the experiments of case 1 with (a) $\sigma = 5$ (solid line) and $\sigma = 10$ (dashed line) and (b) $\sigma = 20$ (solid line) and $\sigma = 40$ (dashed line). The upper-layer curves always have the larger positive values.

of β results in a more unstable flow that extends over a larger fraction of the jet, while the smaller value of k_T allows the eddies to modify the mean shears more easily. Figure 3 shows the mean zonal winds for three values of σ (3, 5, and 10). The upper-level winds have now been reduced from 1.0 in radiative equilibrium to less than 0.6 for the narrowest jet. This is in strong contrast with case 1, in which the upper-level winds increase in strength at the center of the jet. The surface winds are weaker than in case 1 because the momentum fluxes in this model generally decrease in amplitude as β is reduced.

The low-level PV gradient and the PV fluxes for case 2 are shown in Fig. 4. Here, we have included additional calculations for $\sigma = 20$ and 40. The radiative equilibrium PV gradient at the center of the lower layer is now -0.4. The eddies have a larger effect on the minimum value of this gradient than in case 1, but their effect still gets smaller as the jet expands. There is no hint that the fluxes are asymptoting to some constant value as the width increases, unlike case 1, and unlike the one-wave simulations in Panetta and Held (1988). However, the flux is not increasing as fast as σ^2.

To explore the implications of this dependence of the flux on jet width, consider the simplest adjustment hypothesis. We assume that the PV fluxes in the two layers are equal and opposite so that $U_2 = 0$ and

$$\frac{U_{eq} - U_1}{2} = \frac{\partial Q_2}{\partial y} - \frac{\partial Q_{eq}}{\partial y} = -\frac{1}{k_T}\frac{\partial^2 F_2}{\partial y^2}, \quad (10)$$

where

$$\frac{\partial Q_2}{\partial y} = \beta - \frac{U_1}{2}; \quad \frac{\partial Q_{eq}}{\partial y} = \beta - \frac{U_{eq}}{2}. \quad (11)$$

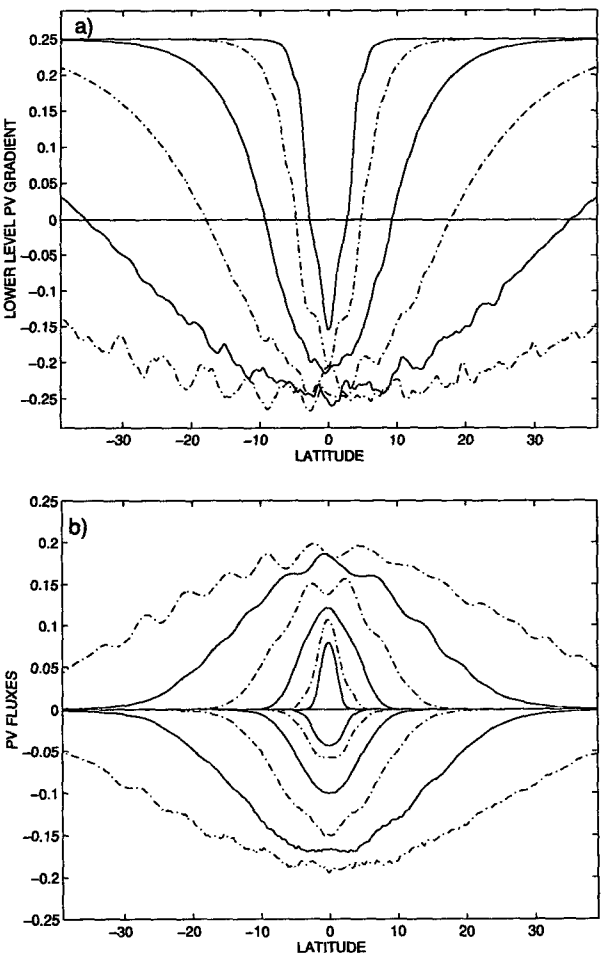

FIG. 2. Meridional profiles of (a) the lower-layer zonal-mean potential vorticity gradient and (b) the eddy potential vorticity flux for the experiments of case 1 with $\sigma = 5$, 10, 20, 40, 80, and 160. In (a) the highest curve corresponds to $\sigma = 5$ and the lowest to $\sigma = 160$. In (b) fluxes increase monotonically in magnitude as σ increases. The upper-layer fluxes are negative, and the lower-layer fluxes positive.

Unauthenticated | Downloaded 07/26/21 04:37 AM UTC

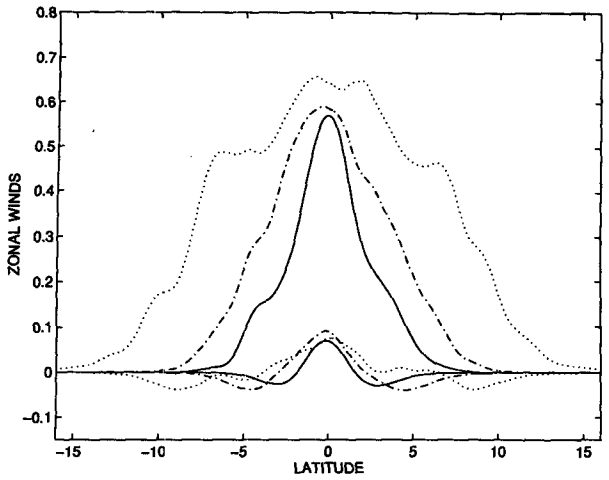

FIG. 3. Meridional profiles of the upper- and lower-layer time-mean zonal-mean wind for the experiments of case 2 with $\sigma = 3$ (solid line), $\sigma = 5$ (dashed line), and $\sigma = 10$ (dotted line).

Setting $Q_{eq} = 0$ at $y = 0$, we can define

$$Q_{eq}(y) = \beta y - \frac{\sigma}{2}\tanh(y/\sigma)$$

$$= \sigma\left(\beta\eta - \frac{1}{2}\tanh(\eta)\right) \quad \eta = \frac{y}{\sigma}. \quad (12)$$

As shown in Fig. 5, the PV gradient in the lower layer is now adjusted to zero between the points at which $Q_{eq}(y)$ crosses zero. This region extends from $-y_c$ to $+y_c$, where $y_c = \alpha\sigma$, and where α is dependent only on β. The PV flux required for this adjustment can be obtained from (10). Its value at $y = 0$ is

$$F_2(0) = \frac{k_T}{2}\int_{-y_c}^{0} Q_{eq}(y)dy = \sigma\frac{k_T}{2}\int_{-\alpha}^{0} Q_{eq}(\eta)d\eta. \quad (13)$$

Since Q_{eq} is proportional to σ, $F_2(0)$ is proportional to σ^2. If one adjusts to a constant negative gradient, rather than zero, the predicted values are reduced, but the flux still increases as σ^2.

As we have seen, as σ increases, the flux is evidently asymptoting to a constant in case 1, while in case 2 the flux continues to increase but less rapidly than σ^2. Consistently, the reduction in the low-level PV gradients in Fig. 4 decreases as σ increases, just as in case 1.

4. Fluxes and diffusivities produced by the homogeneous model

In the homogeneous model, the time-averaged PV fluxes in each layer become horizontally uniform if one integrates long enough. Therefore, we need only examine the domain-averaged PV flux in either layer ($F_1 = -F_2$). For case 1 parameters, and with the prescribed

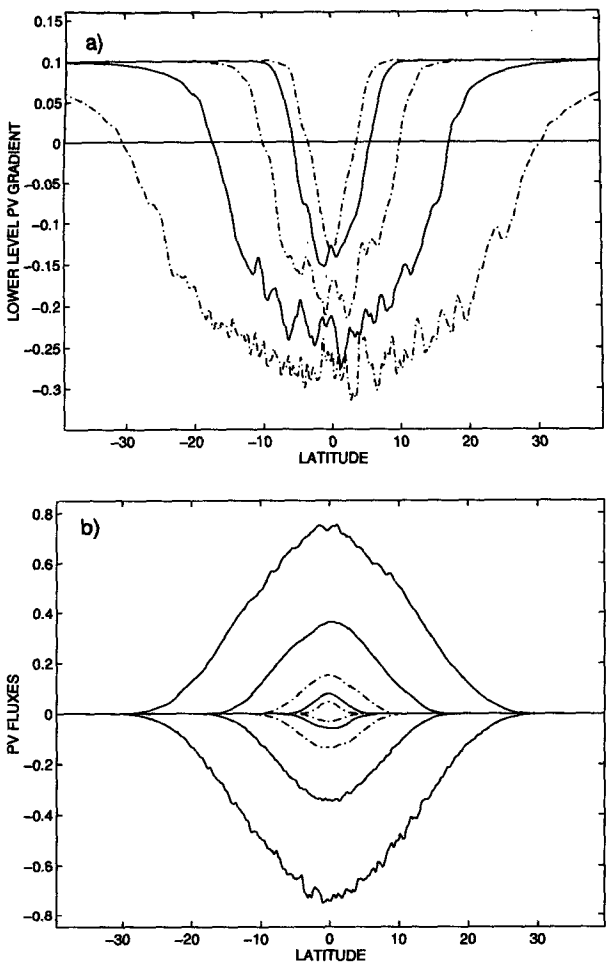

FIG. 4. Meridional profiles of (a) the lower-layer zonal-mean potential vorticity gradient and (b) the eddy potential vorticity flux for the experiments of case 2 with $\sigma = 3$, 5, 10, 20, and 40.

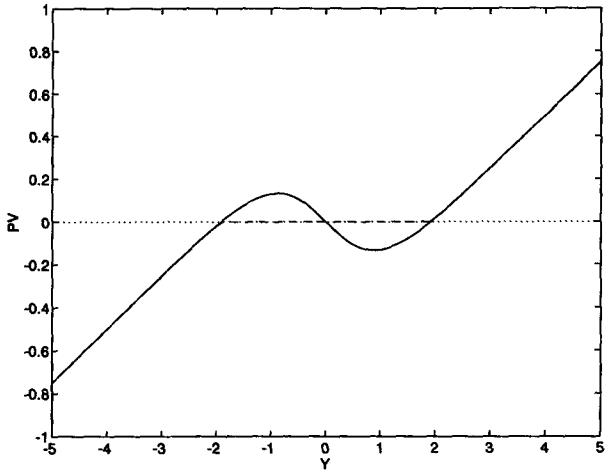

FIG. 5. Meridional profile of the equilibrium (solid line) and of the baroclinically adjusted (dashed line) potential vorticity gradient.

Unauthenticated | Downloaded 07/26/21 04:37 AM UTC

shear $S = U_1 - U_2 = 1$, the resulting PV flux has the magnitude 0.191. This is quite consistent with the value to which the fluxes in the center of the channel seem to be asymptoting in Fig. 2b. Assuming that the eddy fluxes do asymptote to a constant as $\sigma \to \infty$ and that the fluxes vary smoothly with latitude, the eddy flux convergence will approach zero, and the eddies will be incapable of modifying the mean flow. As discussed by Haidvogel and Held (1980) and by Panetta and Held (1988), in this "homogeneous limit" one expects the statistics in the middle of the jet to approach those of the homogeneous model forced by the radiative equilibrium shear at the jet center. This result provides clear evidence for the existence of this asymptotic limit.

Repeating this calculation for case 2 parameters, the homogeneous model predicts a flux of 3.2, which is a factor of 4 larger than the largest values in Fig. 4b. The implication is that we are still far from the homogeneous limit in this case; this limit being much harder to reach than in case 1 because of the larger eddy amplitudes and smaller k_T.

Does this imply that the fluxes predicted by the homogeneous model are relevant only in extraordinarily broad baroclinically unstable flows? To check on their more general relevance, we compute the PV flux in the homogeneous model as a function of the imposed vertical shear S or, equivalently, the lower-layer PV gradient $\beta - S/2$, holding all other parameters fixed. The result is shown in Fig. 6 for cases 1 and 2. One can then consider these curves as a local "theory" for the mean PV flux at a given latitude, given the mean shear or PV gradient.

The validity of this approximation can be determined by the scatterplots in Figs. 7 and 8. We have replotted the homogeneous prediction and superposed a scatterplot of the channel model's low-level PV flux versus its low-level PV gradient. Plotting against shear rather than low-level PV gradient increases the scatter somewhat, but the qualitative result is similar. In case 1, the local homogeneous prediction works remarkably well for all except the narrowest jets, showing clear disagreement only for the two smallest widths, $\sigma = 10$ and 5, for which the homogeneous theory seriously underpredicts the flux. In case 2, the agreement is even better, extending to narrower jets, although the sense of the error in the narrowest case is the same.

These results demonstrate that one can think of the homogeneous model as providing a relation between the local lower-layer PV flux and local PV gradient, $F_2(\partial q/\partial y)$, that can be used to predict the behavior of the inhomogeneous model, except for the narrowest jets. If momentum fluxes are ignored, the nondimensional eddy heat flux H is equal to the lower-layer PV flux and is related to the local vertical shear according to $H(S) = F_2(\beta - S/2)$. This function can be defined by fitting an analytical expression to the points in Fig. 6 or by simply interpolating between these points. One

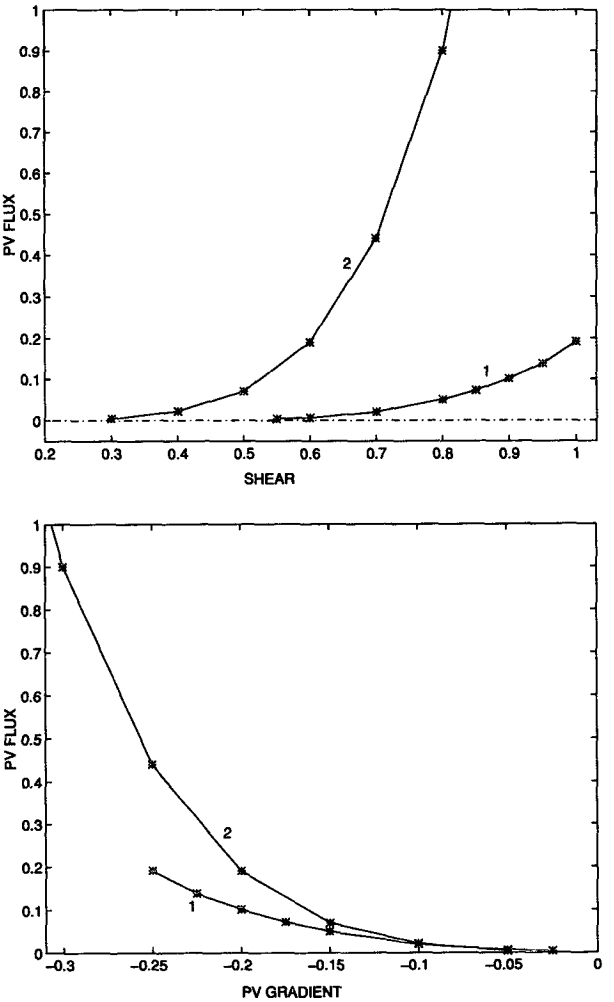

FIG. 6. Domain-averaged lower-layer eddy PV fluxes for the homogeneous model in both case 1 and case 2, as a function of the vertical shear S in the upper panel and as a function of the lower-layer PV gradient in the lower panel (the stars represent the values in each experiment).

can then solve the mean PV or, equivalently, the (nondimensional) temperature equation

$$0 = \frac{\partial \theta}{\partial t} = -\frac{\partial H(S)}{\partial y} - K_T(\theta - \theta_{eq}) \quad \frac{S}{2} = -\frac{\partial \theta}{\partial y}. \tag{14}$$

(Within the quasigeostrophic approximation, there is no transport of heat by the mean meridional circulation if the eddy momentum fluxes are neglected.) The lower-layer PV or heat fluxes that one obtains by solving (14) for different jet widths are displayed in Fig. 9 for the two cases. Here, we have defined the relationship $H(S)$ by linear interpolation on the results in Fig. 6. We have also replotted the lower-layer PV fluxes obtained by integrating the channel model. The results for the narrowest jet in case 1 have not been included

Unauthenticated | Downloaded 07/26/21 04:37 AM UTC

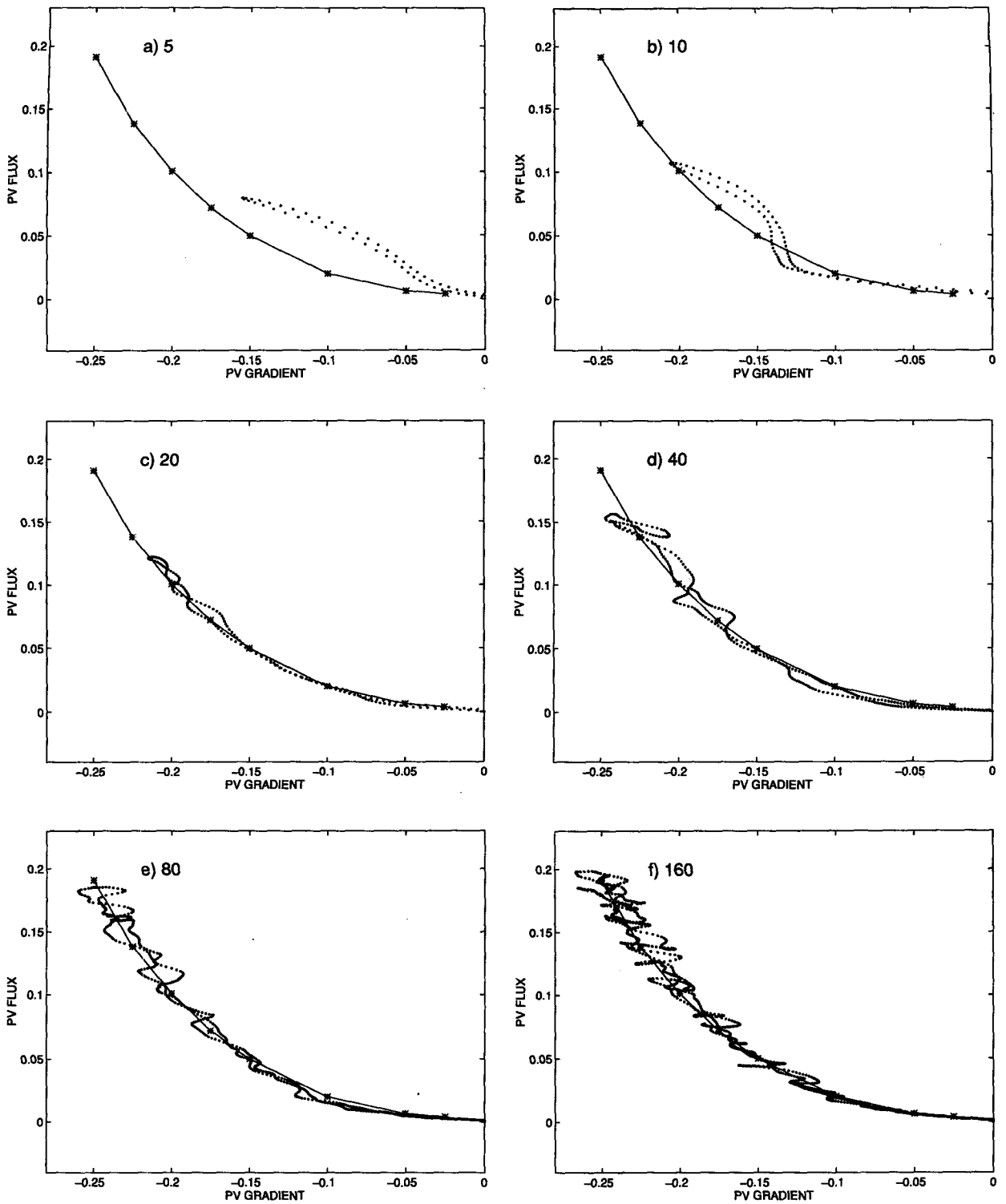

FIG. 7. Comparison between the domain-averaged lower-layer eddy PV fluxes obtained with the homogeneous model as a function of the lower-layer PV gradient (stars and solid line) and the local values assumed by the eddy PV fluxes in the channel experiments as a function of the local PV gradient in the lower layer, for case 1.

Unauthenticated | Downloaded 07/26/21 04:37 AM UTC

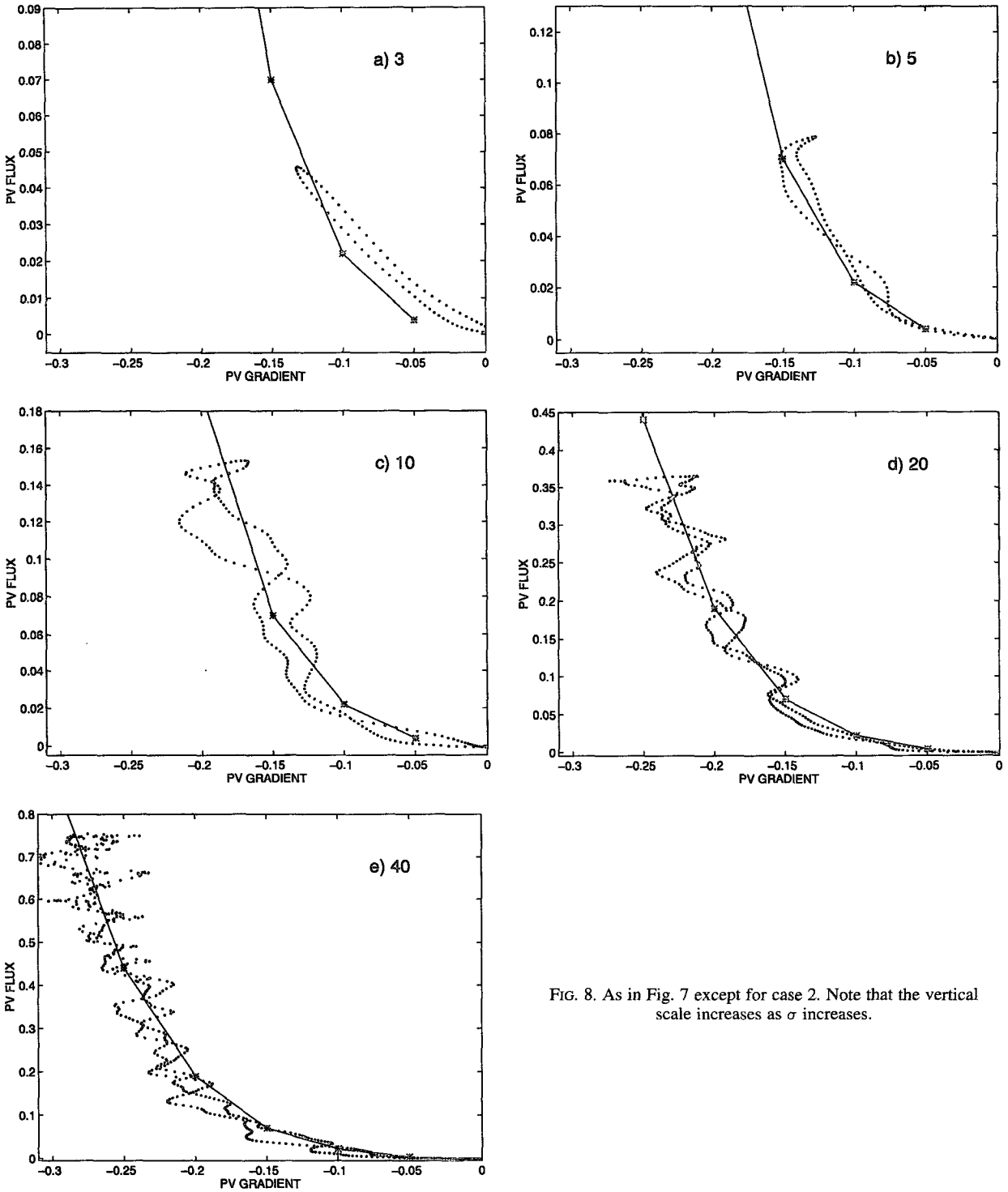

FIG. 8. As in Fig. 7 except for case 2. Note that the vertical scale increases as σ increases.

to avoid conjestion. Consistent with the previous results, this local theory predicts both the meridional distribution and the amplitude of the flux remarkably well, except for narrow jets.

The predicted flux for the narrowest jet in case 1 is plotted in Fig. 10, along with the upper- and lower-layer PV fluxes obtained from the channel model. The sign of the upper-layer flux has been changed. With

Unauthenticated | Downloaded 07/26/21 04:37 AM UTC

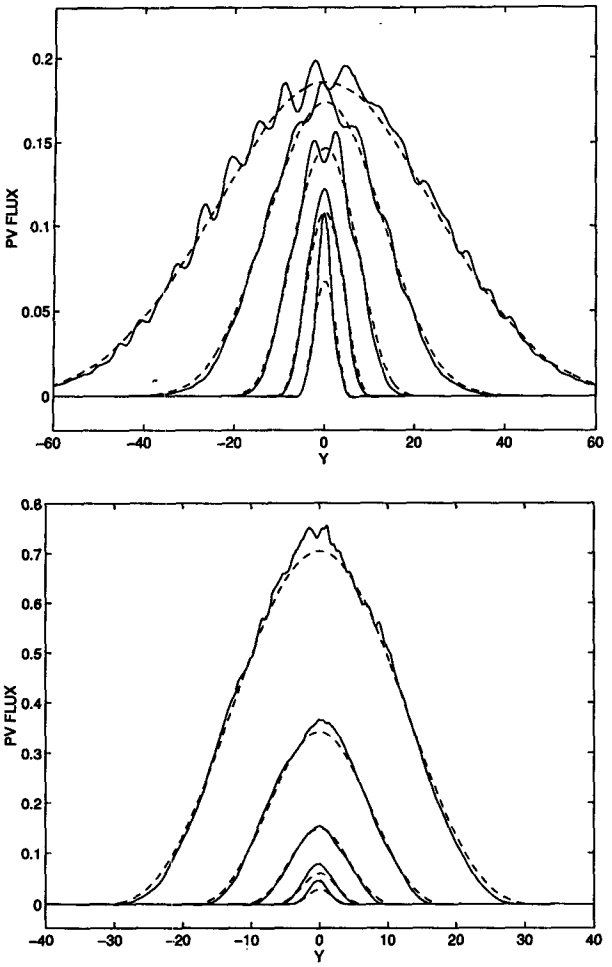

FIG. 9. Meridional profile of the lower-layer eddy PV flux for the channel model (solid lines) and the prediction of the diffusive model described in the text (dotted lines): (upper panel) for case 1 σ = 10, 20, 40, 80, and 160; (lower panel) for case 2 σ = 3, 5, 10, 20, and 40.

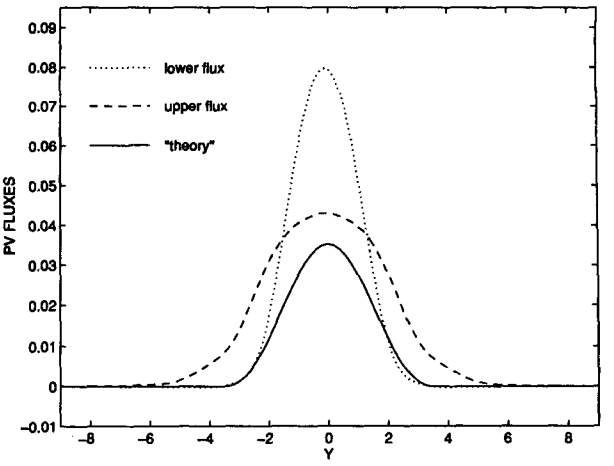

FIG. 10. Meridional profiles of the lower- and upper-layer eddy PV fluxes for the channel model experiment of case 1 with σ = 5, together with the meridional profile of the eddy PV flux predicted by the diffusion model.

this sign change, the eddy heat flux is the average of these two PV fluxes, and the eddy momentum flux convergence is the difference between them. The homogeneous theory cannot distinguish between these different fluxes. It compares somewhat better in amplitude to the upper-layer flux, but the predicted meridional extent agrees better with that of the lower-layer flux. There is no reason to expect detailed agreement between a homogeneous model that has no time-mean momentum flux convergence and a flow in which the eddy momentum fluxes play such a significant role.

We speak of the homogeneous model as providing a local diffusive theory. The PV fluxes predicted by the homogeneous model are downgradient in both layers, except for very weak countergradient fluxes in the lower layer when $S/2 < \beta$. The countergradient flux in these very weakly supercritical flows occurs because of dissipative destabilization (the damping is generating rather than dissipating enstrophy). These small fluxes are of no consequence in the comparison of the homogeneous and inhomogeneous models. To keep the diffusivity well defined, we subtract the small values of the flux when $S = \beta/2$ from the flux at other values of S, before dividing by the PV gradient (in case 1 this value is 0.003). The diffusivities predicted by the homogeneous model in the two layers are not equal, in general; the fluxes are equal and opposite, but the gradients have unequal amplitudes if $\beta \neq 0$.

The diffusivity for lower-layer PV predicted by the homogeneous model is displayed in Fig. 11. Also shown are analytical fits of the form

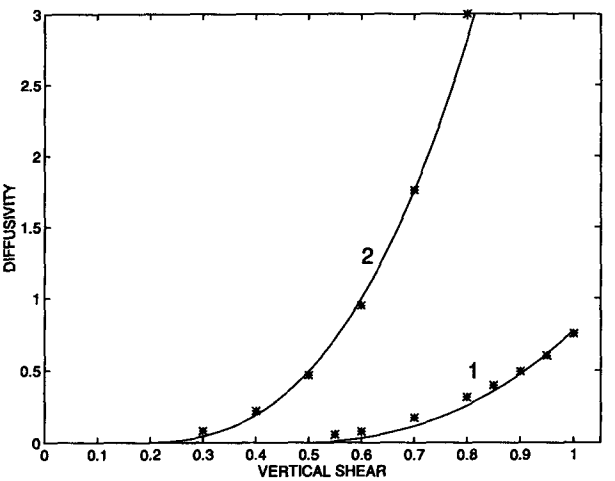

FIG. 11. Diffusivity of the lower-layer PV predicted by the homogeneous model (stars) in cases 1 and 2, and the analytical fit (solid lines), as a function of the vertical shear S.

Unauthenticated | Downloaded 07/26/21 04:37 AM UTC

$$D = \gamma S \xi^{1/2} (\xi - 1)^{3/2}, \quad (15)$$

where

$$\xi \equiv \frac{S}{S_{\text{crit}}}; \quad S_{\text{crit}} \equiv 2\beta.$$

The diffusivity is assumed to drop to zero when S decreases below S_{crit} or, equivalently, when the lower-layer PV gradient becomes positive. The constant γ is set equal to 0.55 in case 1 and 0.34 in case 2. No claim is made as to a physical basis for this fit, although Held and Larichev (1996) argue that $D^*/S\lambda$ should be proportional to ξ^2 in the limit of a very supercritical flow, where D^* is the dimensional diffusivity and λ is the deformation radius. The fit (15) works quite well for the larger fluxes in case 2 produced by shears up to $S = 1$ that are not shown in the figure. A scatterplot of this theory against the diffusivities generated by the integrations of the channel model is similar to that for the fluxes in Figs. 7 and 8 but with more scatter at small values of the PV gradient.

For large shear S, (15) implies that the heat and PV fluxes are proportional to S^4. The fourth-power dependence may seem surprisingly strong, but Held and Larichev describe numerical solutions, more energetic than the flows considered here, that indicate that this fourth-power law actually *underestimates* the sensitivity of the flux to the shear.

If one solves the mean temperature equation (14) with this analytical form for the diffusivity, rather than that obtained by interpolation in Fig. 6, the result is nearly identical to that plotted in Fig. 9.

5. Conclusions

We have integrated a two-layer model of a baroclinically unstable jet to obtain a series of statistically steady states for different jet widths. The simplest baroclinic adjustment construction, in which the lower-level PV gradient is prevented from falling below zero (or some other fixed value), predicts that the eddy PV or heat flux at the jet center should increase in proportion to the square of the width of the jet. This is not found to occur: for one set of parameters studied, the flux clearly asymptotes to a constant as this width increases; for the other (more strongly unstable) set, the flux increases steadily but much slower than the width squared. This is generally consistent with the analogous results with a model truncated to one zonal wave by Panetta and Held (1988), although it appears that the dependence on the width is generally stronger in our isotropically truncated model.

One can try to salvage the adjustment picture by allowing the choice of linear theory, used to determine when the eddies are neutralized, to depend on the flow. For example, following Cehelsky and Tung (1991), one can argue that the eddy energy moves to larger scales as the jet widens and as the flow becomes more energetic and that these eddies are neutralized at larger values of the shear. However, one is then required to predict the scale of the energy-containing eddies. We find it more natural to describe the resulting fluxes with a local diffusive picture, which predicts that the flux asymptotes to a constant as the width increases.

If there is a local relationship between PV fluxes and mean gradients, we argue that a homogeneous turbulence model, of the sort described by Haidvogel and Held (1980), is the appropriate tool for determining this relationship. First of all, by setting the shear in the homogeneous model equal to the radiative equilibrium shear at the center of the jet, this model predicts the maximum PV fluxes that can be expected as the jet width approached infinity. This result explains the difference between the two parameter settings used in the jet computations. In the more weakly unstable case, this homogeneous limit has been nearly attained for the widest jets examined; with the more strongly unstable setting, this maximum flux is still much larger than that found with the jet widths consider here, although it would ultimately be observed if one widened the jets even farther.

More importantly, *the local flux/gradient relationship provided by the homogeneous model explains the magnitude and latitudinal structure of the fluxes in the inhomogeneous baroclinic jet model, even for jets of moderate width in which the mean flow is significantly modified by the eddies.* In the more strongly unstable case, there is good quantitative agreement down to a jet half-width of 3 radii of deformation, in which the half-width of the PV flux itself is roughly 2 radii of deformation.

For the narrowest jets, especially in the more weakly unstable case, this flux–gradient relationship underpredicts the magnitude of the eddy flux. In these cases, the eddy momentum flux convergence, which vanishes in the homogeneous model, is a significant fraction of the PV flux in the upper layer. It would be of interest to determine why the homogeneous theory underpredicts the flux in these cases.

Based on these encouraging results, we believe that diffusive closure schemes for eddy PV (and heat) fluxes can be of great value and that the problem of developing and testing diffusive closure schemes can usefully be split into two parts: 1) computing, and developing a theory for, the fluxes in horizontally homogeneous, baroclinically unstable flows and 2) studying the relationship between the fluxes in these homogeneous flows and the fluxes in inhomogeneous flows of interest, such as baroclinically unstable jets.

Acknowledgments. We would like to thank J. Wittaker, J. Zhang, and V. Larichev for helpful discussion. V. Pavan was supported by Grant NA26RG0102-01 from the National Oceanic and Atmospheric Administration. The views expressed herein are those of the authors

Unauthenticated | Downloaded 07/26/21 04:37 AM UTC

and do not necessarily reflect the views of NOAA or any of its subagencies.

REFERENCES

Cehelsky, P., and K. K. Tung, 1991: Nonlinear baroclinic adjustment. *J. Atmos. Sci.*, **48,** 1930–1947.

Green, J. S. A., 1970: Transfer properties of the large-scale eddies and the general circulation of the atmosphere. *Quart. J. Roy. Meteor. Soc.*, **96,** 157–185.

Haidvogel, D. B., and I. M. Held, 1980: Homogeneous quasi-geostrophic turbulence driven by a uniform temperature gradient. *J. Atmos. Sci.*, **37,** 2644–2660.

Harrison, D. E., 1978: On the diffusion parameterization of mesoscale eddy effects from a numerical ocean experiment. *J. Phys. Oceanogr.*, **8,** 913–918.

Held, I. M., and V. D. Larichev, 1996: A scaling theory for horizontally homogeneous, baroclinically unstable flow on a Beta plane. *J. Atmos. Sci.*, **53,** 946–952.

James, I. N., and L. J. Gray, 1986: Concerning the effect of surface drag on the circulation of a baroclinic planetary atmosphere. *Quart. J. Roy. Meteor. Soc.*, **112,** 1231–1250.

Lee, S., and I. M. Held, 1991: Subcritical instability and hysteresis in a two-layer model. *J. Atmos. Sci.*, **48,** 1071–1077.

Panetta, R. L., 1993: Zonal jets in wide baroclinically unstable regions: Persistence and scale selection. *J. Atmos. Sci.*, **50,** 2073–2106.

——, and I. M. Held, 1988: Baroclinic eddy fluxes in a one-dimensional model of quasi-geostrophic turbulence. *J. Atmos. Sci.*, **45,** 3354–3365.

Phillips, N. A., 1956: The general circulation of the atmosphere: A numerical experiment. *Quart. J. Roy. Meteor. Soc.*, **82,** 123–164.

Smagorinsky, J., 1963: General circulation experiments with the primitive equations I. The basic experiment. *Mon. Wea. Rev.*, **91,** 99–164.

Stone, P. H., 1978: Baroclinic adjustment. *J. Atmos. Sci.*, **35,** 561–571.

Vallis, G. K., 1988: Numerical studies of eddy transport properties in eddy-resolving and parameterized models. *Quart. J. Roy. Meteor. Soc.*, **114,** 183–204.

Wiin-Nielsen, A., and J. Sela, 1971: On the transport of quasi-geostrophic potential vorticity. *Mon. Wea. Rev.*, **99,** 447–459.

Unauthenticated | Downloaded 07/26/21 04:37 AM UTC